This article is published as part of a themed issue of ***Photochemical & Photobiological Sciences*** in honour of

Jan Verhoeven

Guest edited by **Anthony Harriman**

Published in **issue 7, 2010**

Communication

Papers

A photo- and electrochemically-active porphyrin–fullerene dyad electropolymer†‡

Miguel Gervaldo,[b] Paul A. Liddell,[a] Gerdenis Kodis,[a] Bradley J. Brennan,[a] Christopher R. Johnson,[a] James W. Bridgewater,[a] Ana L. Moore,*[a] Thomas A. Moore*[a] and Devens Gust*[a]

Received 29th January 2010, Accepted 15th March 2010
First published as an Advance Article on the web 1st April 2010
DOI: 10.1039/c0pp00013b

A hole- and electron-conducting polymer has been prepared by electropolymerization of a porphyrin–fullerene monomer. The porphyrin units are linked by aminophenyl groups to form a linear chain in which the porphyrin is an integral part of the polymer backbone. The absorption spectrum of a film formed on indium-tin-oxide-coated glass resembles that of a model porphyrin–fullerene dyad, but with significant peak broadening. The film demonstrates a first oxidation potential of 0.75 V *vs.* SCE, corresponding to oxidation of the porphyrin polymer, and a first reduction potential of –0.63 V *vs.* SCE, corresponding to fullerene reduction. Time-resolved fluorescence studies show that the porphyrin first excited singlet state is strongly quenched by photoinduced electron transfer to fullerene. Transient absorption investigations reveal that excitation generates mobile charge carriers that recombine by both geminate and nongeminate pathways over a large range of time scales. Similar studies on a related polymer that lacks the fullerene component show complex, laser-intensity-dependent photoinduced electron transfer behavior. The properties of the porphyrin–fullerene electropolymer suggest that it may be useful in organic photovoltaic applications, wherein light absorption leads to charge separation within picoseconds in a "molecular heterojunction" with no requirement for exciton migration.

1. Introduction

In biology, porphyrins and their relatives the chlorophylls play a wide variety of important roles, most of which depend on the redox properties of these macrocycles and/or their interactions with light. These same properties of synthetic porphyrins are exploited through applications in solar energy conversion, sensors, biomedicine, molecular electronics and photonics. When porphyrins are used in a device, it is often necessary to transduce a redox change in a porphyrin molecule into an electrical response at an electrode. One convenient way to do this is to include the porphyrin in an electrically conducting polymer film grown electrochemically on an electrode surface. A variety of porphyrin-containing electropolymers have been reported.[1–7] In these, polymerization occurs *via* substituents attached to the porphyrin ring, rather than through the carbon atoms of the macrocycle itself. Porphyrin electropolymers based on polyaniline are especially well studied.[1,2,6,8] The groups of Spiro and of Murray and other investigators have reported the electropolymerization of 5,10,15,20-tetrakis(2-aminophenyl)porphyrins,[9–15] and found that they polymerize oxidatively *via* the *meso* aniline rings in a head-to-tail fashion in much the same way as aniline itself. Due to the presence of four aminophenyl groups on each macrocycle, the porphyrin units can bridge between polyaniline chains. The resulting material is essentially a form of polyaniline with attached porphyrin moieties. Hole conductivity in these polymers can thus occur in ways similar to conduction in polyaniline, although the porphyrin ring could be involved in interchain hopping.

Recently, we reported[16] a new kind of porphyrin polymer, **poly1**, which is prepared by electropolymerization of 5-(4-aminophenyl)-10,20-bis(2,4,6-trimethylphenyl)porphyrin, **1** (Fig. 1). Polymerization occurs *via* bonding of the aminophenyl nitrogen directly to the carbon atom at the 15-position of the porphyrin ring, leading to a structure in which the porphyrin macrocycle is an integral part of the linear, conjugated, semiconducting polymer backbone (Fig. 2). Preliminary optical and electrical studies of these conducting porphyrin films suggest that they might be useful for photovoltaic and/or sensing applications.

Natural photosynthetic reaction centers, responsible for conversion of excitation energy into useful chemical energy, can serve as inspiration for construction of solar energy conversion devices. In reaction centers, the energy conversion step involves electron donation from a chlorophyll first excited singlet state, formed by light absorption, to a nearby electron acceptor species to form a charge-separated state. This state preserves some of the original photon energy as electrochemical potential energy. We and others have reported many examples of artificial photosynthetic reaction centers that consist of porphyrins covalently linked to quinones, fullerenes, porphyrins, or other electron-accepting moieties. Some

[a]*Department of Chemistry and Biochemistry, Center for Bioenergy and Photosynthesis, Arizona State University, Tempe, AZ, 85287, USA. E-mail: amoore@asu.edu, tom.moore@asu.edu, gust@asu.edu*
[b]*Departamento de Química, Universidad Nacional de Río Cuarto, Agencia Postal 3 (5800), Río Cuarto, Argentina*

† This article is published as part of a themed issue in appreciation of the many important contributions made to the field of molecular photophysics by Jan Verhoeven.

‡ Electronic supplementary information (ESI) available: Synthesis and characterization of new compounds, experimental details for electrochemical and spectroscopic studies, Fig. S2 showing transient absorption kinetics at 880 nm for **poly1** on ITO-coated glass. See DOI: 10.1039/c0pp00013b

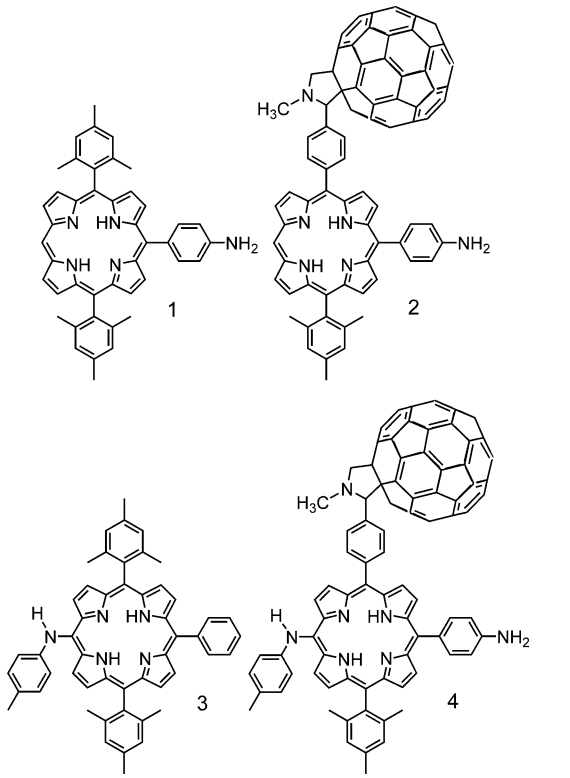

Fig. 1 Structures of monomers porphyrin **1** and porphyrin–fullerene dyad **2**, and of model compounds porphyrin **3** and dyad **4**.

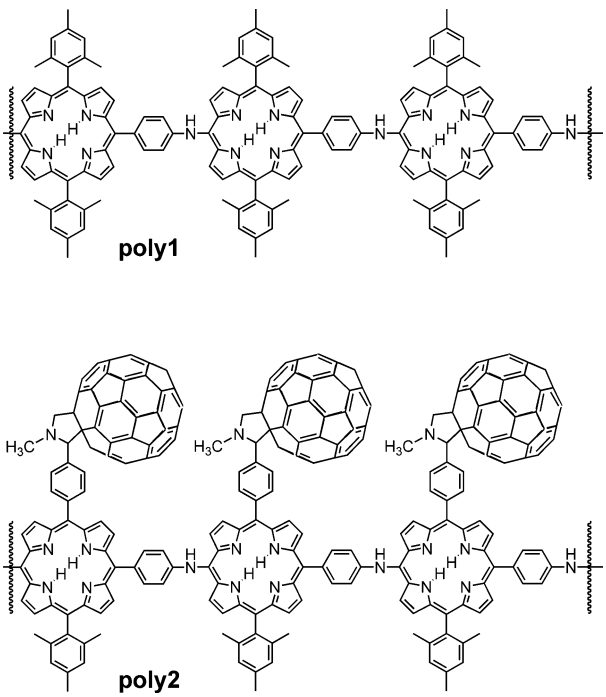

Fig. 2 Structures of the electropolymers **poly1** and **poly2**.

of these dyads, triads, *etc.* rival natural reaction centers in their ability to store energy from light in energetic, long-lived charge-separated states in high yield.[17–26]

These results suggest that a promising approach to the design of polymers for solar energy conversion purposes would be to include similar dyad photochemical charge-separation units in the polymer chain. In this way, light absorption by any unit in the polymer could be followed by rapid photoinduced electron transfer to form a charge separated state. Subsequent electron and hole migration through the polymer to electrodes could generate photocurrents and photovoltages. Thus, each unit of the polymer would form a "molecular heterojunction" wherein a Frenkel exciton (excited state) formed by light absorption could dissociate into carriers, and the exciton migration required by many approaches to the design of polymer-based solar energy conversion devices, which can lead to decreased efficiencies, would be unnecessary. A few polymers bearing both electron and hole carriers, sometimes termed "double cable" polymers, have been reported and evaluated for solar energy conversion purposes.[27–29] Most designs consist of light-harvesting conjugated polymers (but not porphyrins) tethered to electron acceptors such as fullerenes.

Herein we report electropolymer **poly2** (Fig. 2), which is an analog of **poly1** in which each porphyrin unit bears an appended fullerene electron acceptor moiety. The polymer is formed by electropolymerization of monomeric dyad **2** (Fig. 1) under conditions similar to those used for **1**.

2. Results

2.1 Synthesis of the monomer

The syntheses of monomer **1** and model porphyrin polymer unit **3** (Fig. 1) were reported previously.[16] Monomer **2** was prepared from 5-(4-formylphenyl)-15-(2,4,6-trimethylphenyl)porphyrin. One free *meso* position was brominated, and the bromine was replaced by the 4-aminophenyl group (protected as the BOC derivative) *via* a Suzuki-type coupling. The fullerene was then attached through a Prato reaction with the porphyrin aldehyde, sarcosine and C_{60}. Finally, the BOC protecting group was removed with trifluoroacetic acid to give **2**. Model compound **4** (Fig. 1) was prepared in a related fashion. The synthetic details and characterization by NMR and mass spectrometry are given in the ESI.‡

2.2 Electrochemistry

Cyclic voltammetry (CV) of **2** in dry, deoxygenated dichloromethane containing 0.10 M tetra-n-butylammonium hexafluorophosphate supporting electrolyte was carried out using a platinum disk working electrode, a platinum counter electrode, and a Ag/AgCl quasi-reference electrode (Fig. 3). The electrochemical reduction shows three reversible one electron processes between 0 and –1.5 V *vs.* SCE. The two first reductions, at –0.61 and –0.99 V, correspond to the formation of the mono- and dianion of the C_{60} unit respectively,[30] and the third one at –1.20 V is due to porphyrin anion formation. The first anodic sweep also presents three oxidation waves (I, II, III in Fig. 3). The complementary reduction peaks are all absent in the reverse sweep, indicating that the oxidation processes are irreversible. On the reverse sweep, two reduction peaks are observed near 0.66 and 0.46 V. They are assigned to the reduction of the product/products generated during the first oxidation sweep. For purposes of comparison, we note that the CV of 5,10,15,20-tetraphenylporphyrin in benzonitrile features oxidation waves at

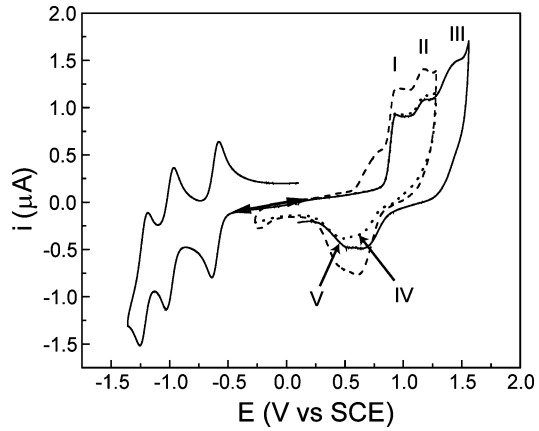

Fig. 3 Cyclic voltammograms for **2** in dry, deoxygenated dichloromethane containing tetra-n-butylammonium hexafluorophosphate. The scan rate was 0.1 V s^{-1}. The arrows indicate the initial scan directions for the anodic and cathodic sweeps. The solid lines represent the initial cathodic and anodic scans. The dotted line is an initial anodic sweep between –0.25 V and 1.27 V, and the dashed line is a second anodic sweep of the same electrode. See the text for an explanation of the Roman numerals.

1.08 and 1.23 V *vs.* SCE,[31] and the first oxidation potential of aniline in acetonitrile is 0.90 V *vs.* SCE.[32]

When a solution of **2** is scanned between –0.25 and 1.27 V only two oxidation peaks are observed, corresponding to waves I and II, and the complementary reduction peaks are still not observed. Instead, two reduction peaks can again be seen at 0.66 and 0.46 V (peaks IV, V, dotted line, Fig. 3). On the second scan over this potential range, a new peak is observed at ~0.75 V. It occurs at a less positive potential than that for wave I. Also a second peak is observed in the same region as the first and second oxidation processes. The reduction waves IV and V and the new oxidation peaks are evident only after the first anodic sweep; hence, they are generated *via* a chemical reaction following the initial oxidations of **2**.

Fig. 4 shows successive anodic CV curves of a dichloromethane solution of **2**, prepared as described above and cycled between –0.25 V and through the second oxidation wave to 1.3 V. The voltammograms show a progressive increase in total current with each sweep, indicating the formation of a redox-active material on the electrode. In addition, new peaks grow in as the number of cycles increases. After about 20 cycles, a single broad wave dominates the CV. A similar film is also formed when the monomer solution is cycled between 0 V and the third oxidation, but lower coverage is obtained. At the end of the process, the electrode is seen to be covered with a relatively uniform polymeric film.

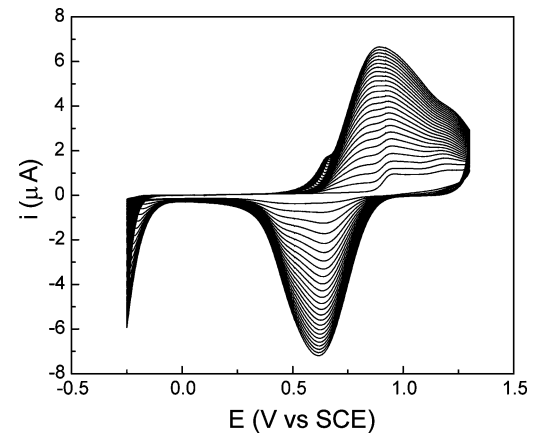

Fig. 4 Cyclic voltammograms showing repetitive anodic cycles for a solution of **2** as described for Fig. 3. Each successive cycle has a higher current. A total of 25 cycles are shown.

When the polymer-coated Pt electrode is removed from the monomer solution, rinsed with dichloromethane, and transferred to a new solution of electrolyte containing no monomer, it shows the redox responses depicted in Fig. 5. The cyclic voltammogram of the film presents a broad reversible oxidation at 0.75 V (calculated as the average of the anodic and cathodic peaks) showing a nearly symmetrical current response but with a peak separation larger than predicted for an ideal process at these scan rates. This oxidation potential is close to that observed for similar polymer films of **poly1** (0.85 V *vs.* SCE),[16] and is assigned to oxidation of the polymeric porphyrin. The reductions of the polymer occur at –0.63, –0.97 and –1.12 V *vs.* SCE. The reductions at –0.63 and –0.97 are essentially identical in potential to those observed for the fullerene component of **2**, and are assigned to the C_{60} moiety. The reduction at –1.12 is assigned to the porphyrin macrocycle, and is identical to the value reported for reduction of **poly1**.[16] At scan rates in the 10–200 mV s^{-1} range, the amplitudes of both the oxidation and reduction current peaks are proportional to the scan rate, which is indicative of an irreversibly adsorbed product on the electrode.[33]

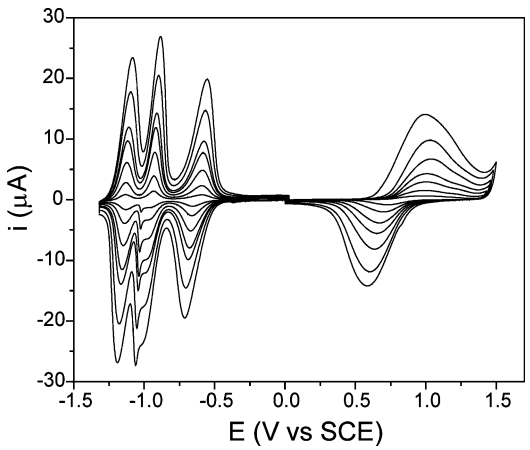

Fig. 5 Cyclic voltammograms as a function of scan rate for a film of **poly2** obtained after 25 CV cycles. The conditions were the same as indicated in Fig. 3 except that the solution did not contain monomeric **2**. The scan rates (larger amplitude to smaller) were 200, 150, 100, 75, 50, 25 and 10 mV s^{-1}.

The film shows "memory" effects when the potential is scanned over certain ranges. The solid line in Fig. 6 shows the CV of a film of **poly2** on platinum taken for a complete cycle of potentials from –0.75 V to 1.50 V, and then back to –0.75 V. The dotted lines show cycles between 0.00 and –0.75 V, and between 0.00 and 1.50 V. Note that the full cycle contains features near 0.75 V and –0.30 V that do not appear in the simple reductive or oxidative scans. Such sharp prewaves, or "trapping peaks" have been observed in other polymers, and commonly occur in electropolymers that have multiple redox processes separated widely in potential.[33,34] They may be ascribed to redox processes that have a formal

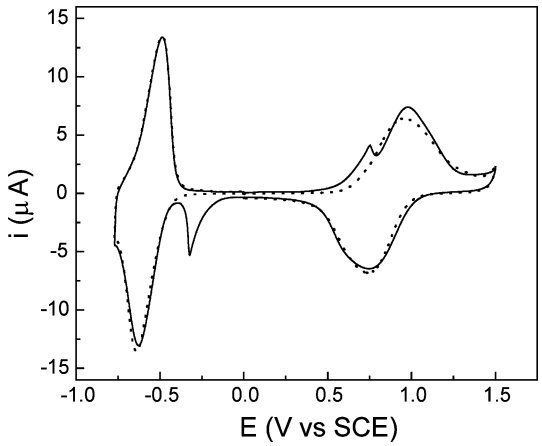

Fig. 6 Cyclic voltammograms of a film of **poly2** on a platinum electrode in 0.1 M tetra-n-butylammonium hexafluorophosphate in dichloromethane solution scanned at 100 mV s^{-1}. The solid line was obtained by scanning a continuous, full cycle between the potential limits of –0.75 V and 1.5 V *vs.* SCE, and back. The two dotted lines show scans between 0 V and –0.75 V and between 0 V and 1.5 V.

potential lying within one of the major conductive zones. When these redox sites fail to discharge before the sweep through the relevant conductive zone is finished, they will not discharge until the next conductive zone is reached. Such behavior is also seen when there are states that have a formal potential in the insulating voltage region. These states oxidize within one conductive region and are reduced in the other.

2.3 Mass spectrometry

The structure of **poly2** is postulated to be similar to that of **poly1**, whose structure was determined based on a number of techniques.[16] MALDI-TOF negative ion mode mass spectrometric results for **poly2** were consistent with this assignment, within experimental error. Samples of the essentially insoluble polymer were scraped from the substrate and sonicated with a terthiophene matrix. For **2**, the molecular formula $C_{104}H_{38}N_6$ yields calculated values for m/z and $(m + 1)/z$ of 1370.32 and 1371.32, respectively. Experimental reflective mode measurements gave major peaks for **poly2** with roughly equal abundance at 1370.06 and 1371.06. The **poly2** sample also showed a dimeric species. Calculations of m/z and $(m - 1)/z$ for the neutral dimer $C_{208}H_{74}N_{12}$ yield 2740.62 and 2739.62. Experimental masses of approximately equal intensity were found at 2740.41 and 2739.41. In linear mode, a peak at 4106 was observed. The exact mass for the trimer $C_{312}H_{110}N_{18}$ is 4106.92 and the molecular weight is 4110.

2.4 Spectroscopic properties—absorption spectra

Electropolymerization of **2** was also carried out on transparent electrodes consisting of a thin layer of indium tin oxide (ITO) or fluorinated tin oxide (FTO) on glass. The polymerization proceeds as it does on platinum, and the CVs show similar increases in current and changes in shape as each cycle is completed. After removal of the electrode from the polymerization solution, washing with dichloromethane and re-immersion in a clean electrolyte solution, the electrode gives cyclic voltammograms showing similar redox potentials and shapes to those for films grown on a platinum electrode.

Fig. 7 shows the absorption spectra of **2** and **3** in dichloromethane solution and of an electrode bearing a film of **poly2** (30 polymerization cycles) in air. The spectrum of the polymer was corrected for scatter by the FTO electrode by subtraction of the spectrum of the electrode prior to polymerization. The spectrum of **2** features the porphyrin Soret band absorption at 415 nm and four Q bands at 510, 545, 585, and 640 nm. The fullerene moiety shows weak, featureless absorption all through the visible region out to 705 nm, where a weak maximum is observed. The spectrum of porphyrin **3**, a better model compound for the porphyrin moiety of **poly2**, has maxima at 421, 520, 570, 590 and 664 nm. The spectrum of the film of **poly2** also shows Soret, Q-band and C_{60} absorptions. All the bands are strongly broadened and red shifted relative to those of the model compounds (the Soret band shifts to 434 nm). The spectrum indicates that the component chromophores are basically unaltered by polymerization; the red shifts and spectral broadening are characteristic of chromophore association (with possible excitonic coupling and formation of charge-transfer states) and environmental heterogeneity in the film. Excited states (excitons) are self-trapped, and any excited state motion would likely occur by hopping. If the film is "doped" by the presence of some oxidized porphyrin, additional absorbance is observed, especially at wavelengths longer than 650 nm (*vide infra*).

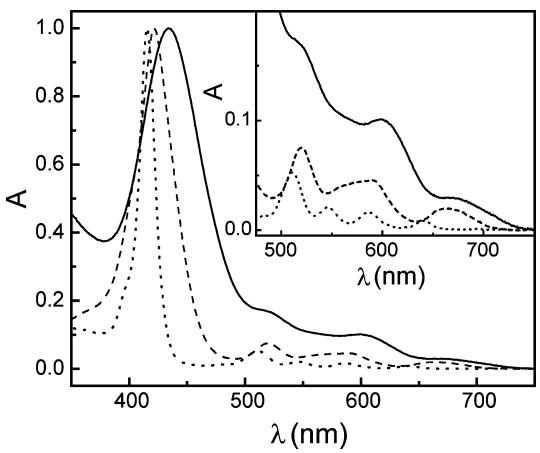

Fig. 7 Absorption spectra of (dotted line) monomer **2** in dichloromethane solution, (dashed line) model porphyrin **3** in dichloromethane solution, and (solid line) **poly2** on FTO in air (30 polymerization cycles). For comparison purposes, the absorbance values are normalized at the Soret maximum. The inset is an expansion of the long-wavelength region.

2.5 Spectroelectrochemical studies

The **poly2** film readily undergoes oxidation and reduction, as demonstrated by the CV results. By analogy with porphyrin–fullerene dyads related to **2** or **4** in solution, excitation of the porphyrin or fullerene moieties of **poly2** is expected to be followed by photoinduced electron transfer to yield $P^{\bullet+}$–$C_{60}^{\bullet-}$ charge-separated states.[35–40] For these reasons, spectroelectrochemical studies were performed to obtain information about the species resulting from oxidation and reduction of the film. An electrode bearing an electropolymerized film of **poly2** on ITO-coated glass,

prepared as described above, was immersed in dichloromethane containing 0.1 M tetra-n-butylammonium hexafluorophosphate. The electrode was set at 0.0 V *vs.* SCE in the electrochemical cell, and its UV-visible absorption spectrum was recorded and baseline-corrected using a blank ITO electrode. The potential was then set at –0.75 V in order to convert the film to its reduced state (first reduction), and the absorption spectrum was again obtained. Fig. 8 shows the difference spectrum obtained by subtracting the spectrum at 0.0 V from that at –0.75 V. The difference spectrum features a strong band with a maximum at 1006 nm, with some lower amplitude features at shorter wavelengths. The 1006 nm band is ascribed to the fullerene radical anion by reference to similar compounds.[41] Fig. 8 also shows the difference spectrum obtained after a similar potential-controlled (–0.75 V) electrolysis of a solution of **2** in dichloromethane/tetra-n-butylammonium hexafluorophosphate. The spectrum resembles that for **poly2**, with an absorption maximum at 995 nm that is ascribed to P–$C_{60}^{\bullet-}$.

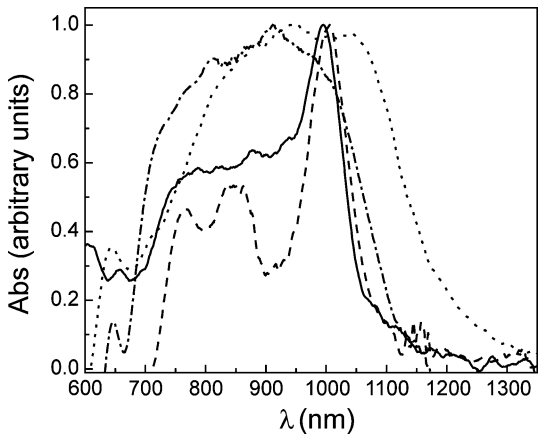

Fig. 8 Spectroelectrochemical difference spectra. Films were prepared on ITO-coated glass and spectra were obtained from electrodes in dichloromethane solution containing supporting electrolyte as discussed in the text. The dashed line shows the difference spectrum for a film of **poly2** taken at the first reduction, –0.75 V, and the solid line shows a similar difference spectrum for monomeric **2** in the same solvent and electrolyte. The dotted line is the difference spectrum for the **poly2** film after the first oxidation (1.25 V), and the dot-dash line is the corresponding difference spectrum for **poly1**. The spectra have been normalized to a maximum absorbance of 1.0 to facilitate comparison.

Turning now to oxidative conditions, a UV-visible absorbance difference spectrum of the **poly2** film was obtained after poising the electrode at a potential of 1.25 V, which converts the film to its first oxidized state. As shown in Fig. 8, a broad, featureless absorption in the 700–1250 nm region was observed. A similar difference spectrum was obtained from a film of **poly1**, with a broad absorption in the 600–1100 nm region (Fig. 8). For both polymers, this band is assigned to the porphyrin radical cation. The radical cation of related monomeric porphyrins in solution also has a broad, featureless spectral signature, but it is usually found in the 600–900 nm region.

2.6 FT-IR studies and film permeability

During the CV experiments described above, a large fraction of the P–C_{60} units in the polymer is being oxidized or reduced in the high-current regions of the voltammogram. If the interior of the polymer film is accessible to ions in the electrolyte solution, then oxidation or reduction of the film is expected to be accompanied by migration of counterions into the film. In order to investigate this possibility, films of **poly2** were grown on ITO-coated glass in dichloromethane using tetra-n-butylammonium hexafluorophosphate as the supporting electrolyte, the films were removed from the polymerization solution and rinsed with dichloromethane, and the films were then immersed in a clean dichloromethane solution of the same electrolyte. The electrode potential was set at various values to convert the film to a particular oxidation state, and the film was removed from the electrolyte and rinsed with dichloromethane. The infrared spectrum of the electrode was then taken using the Fourier-transform technique. The results appear in Fig. 9a. Oxidation of the film at 0.5, 0.8 and 1.2 V *vs.* SCE is accompanied by increases in the absorption by a band at 845 cm^{-1}. This band is in the range typically observed for PF_6^-. Thus, as the degree of oxidation of the film is increased, PF_6^- ions migrate into the film to compensate the positive charge. When similar experiments were carried out with tetra-n-butylammonium perchlorate as the supporting electrolyte, the spectra in Fig. 9b

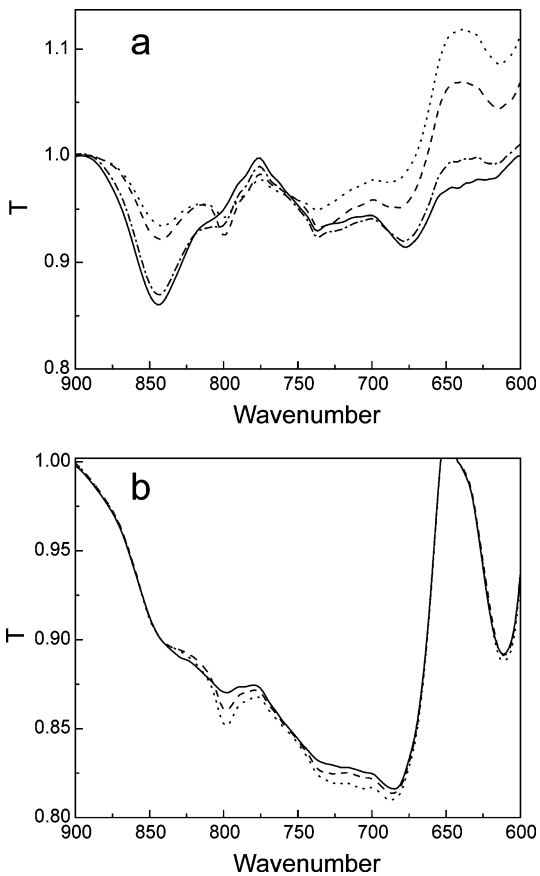

Fig. 9 FT-IR spectra of the electropolymers. (a) Film of **poly2** on ITO covered glass, taken *in vacuo*, after oxidation in a solution of dichloromethane containing 0.10 M tetra-n-butylammonium hexafluorophosphate at potentials of 0.0 V *vs.* SCE (dot), 0.5 V (dash), 0.8 V (dot-dash) and 1.2 V (solid). Note the increase in absorbance due to the PF_6^- vibration at 845 cm^{-1} with increasing potential. (b) Similar film prepared in dichloromethane containing 0.10 M tetra-n-butylammonium perchlorate at potentials of 0.0 V *vs.* SCE (dot), 0.5 V (dash), and 1.0 V (solid). The 845 cm^{-1} band is absent.

were obtained. The 845 cm^{-1} peak is absent, and only a small decrease in the 840 cm^{-1} region is observed as the oxidation state of the polymer is increased. On the other hand, increasing the degree of oxidation does result in an increase in the perchlorate band at 1100 cm^{-1} (data not shown). Thus, the film is permeable to solvent and these counterions.

2.7 Film thickness

The thickness of polymer films grown on FTO-coated glass as described above was determined by profilometry using a Sloan Dektac II Profilometer. Fig. 10a shows a plot of the film thickness *vs.* absorbance at the Soret band maximum for **poly2** films of various thickness. The least-squares best fit to these data (Fig. 10a) yields 74 nm per absorbance unit. Fig. 10b shows similar data for **poly1**. In this case, the best fit gives 101 nm per absorbance unit. The thickness of a film of **poly1** was estimated previously using a focused ion beam technique to cut the film, coupled with scanning electron microscopy (SEM). Films of two thicknesses were studied, and based on these data, the film was estimated as ~150 nm per absorbance unit at the Soret maximum.[16] The estimates from the two techniques are consistent, given the experimental errors in each set of measurements. Similar SEM studies on a sample of **poly2** also yielded results comparable to the profilometry measurements (solid circle in Fig. 10a). For **poly1**, SEM and atomic force microscopy measurements both showed that the film was relatively smooth and uniform. The films of **poly2** show reasonably uniform UV-vis absorbance over the slide, suggesting that these films are also uniform in thickness. The SEM data on **poly2** are consistent with this conclusion.

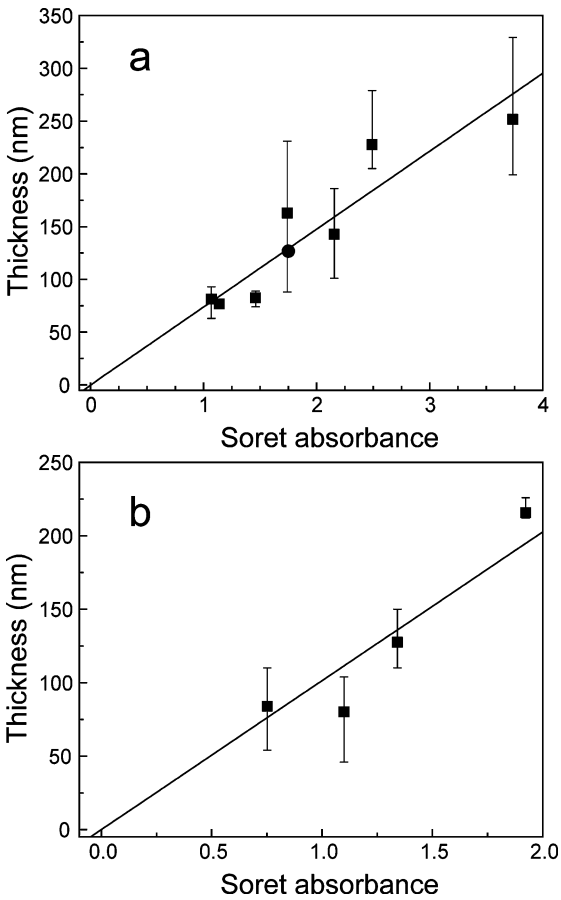

Fig. 10 Film thickness as determined by profilometry *vs.* the absorbance at the Soret maximum in the UV-visible spectrum (solid squares): (a) films of **poly2** (the solid circle is a result from SEM measurements); (b) films of **poly1**. The lines are linear least-squares best fits to the profilometry data. The error bars show the range of results obtained for multiple experiments.

The density of **poly2** particles scraped from an electrode was determined by the flotation method to be 1.53 ± 0.05 g mL^{-1}. Based on this density and the relationship from Fig. 10a, the extinction coefficient at the Soret maximum (434 nm) is $121\,000 \pm 4000$ M^{-1} cm^{-1} per dyad unit in the film. This extinction coefficient is roughly one-quarter of those typically found for *meso*-triarylporphyrins, which is reasonable given that the Soret band of **poly2** is about 4 times broader than that of monomer **2**, based on the width at half height. The density estimate indicates that the volume per dyad repeat unit in **poly2** is 1490 $Å^3$. This estimate appears reasonable, as the van der Waals volume of one monomer unit, based on an MM2 molecular mechanics structure minimization, is 1100 $Å^3$. Based on the estimated volume per dyad, roughly approximating the dyad repeat unit as a cube of 11.5 Å implies that there are *ca.* 87 dyad repeat units between the surfaces of a 100 nm film.

For **poly1**, the density was found to be 1.42 ± 0.05 g mL^{-1}. From this density and the relationship in Fig. 10b, the extinction coefficient at the Soret maximum is $44\,350 \pm 1500$ M^{-1} cm^{-1} per dyad unit in the film. The extinction coefficient is significantly lower for **poly1** than for **poly2**. It is unlikely that the entire difference is accounted for by the contribution from the fullerene in **poly2**. Examination of the absorption spectrum[16] of **poly1** shows that the Soret band is roughly 5.3 times broader than the corresponding band in the monomer **1**, which is consistent with a lower extinction coefficient at the maximum. However, for both **poly1** and **poly2** films, band widths and oscillator strengths depend on the details of the excitonic coupling interactions between porphyrins in the same and different polymer strands. The density estimate for **poly1** indicates that the volume for each dyad repeat unit is 744 $Å^3$, whereas the van der Waals volume of a monomer unit based on an MM2 calculation is 605 $Å^3$. For **poly2** the experimental volume per repeat unit is 1.36 times larger than the van der Waals volume, and for **poly1** the corresponding number is 1.23, suggesting that in both films the amount of "vacant" space available for solvent, counterions, *etc.* is roughly the same fraction of the amount of space occupied by polymer units. Based on the estimated volume of **poly1** per repeat unit, approximating the repeat unit as a cube with dimensions of 9.1 Å implies that there are *ca.* 110 repeat units between the surfaces of a 100 nm film.

2.8 Transient spectra

As mentioned above, a salient characteristic of porphyrin–fullerene dyads is photoinduced electron transfer. In order to investigate this possibility in **poly2** we used transient emission and absorption techniques. Model compound **4** is a porphyrin and fullerene dyad closely related to those in a single unit of the polymer. Unlike the typical porphyrin, the porphyrin moiety of **4** has essentially no steady-state fluorescence emission, showing that the porphyrin first excited singlet state is strongly quenched. A sample of **4** was dissolved in 2-methyltetrahydrofuran and its transient absorption properties were studied using the pump–probe

technique with excitation at 590 nm, where the porphyrin absorbs most of the light. Some results are shown in Fig. 11.

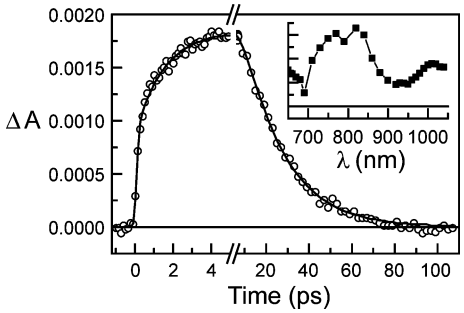

Fig. 11 Transient absorption results for model dyad **4** in 2-methyltetrahydrofuran solution following excitation at 590 nm with a *ca.* 100 fs laser pulse. The inset shows the spectrum 5 ps after excitation, which is characteristic of the porphyrin radical cation and fullerene radical anion. The circles show the rise and decay of the absorbance at 1000 nm. Fitting these data (solid lines) yields a prompt rise due to formation of ^{1}P, a slower rise with a time constant of 4.0 ps reflecting formation of $P^{\bullet+}$–$C_{60}^{\bullet-}$ by photoinduced electron transfer, and a decay (20 ps) representing recombination of the charge-separated state.

The inset is a spectrum taken 5 ps after excitation, and shows induced absorbance with maxima around 800 and 1010 nm. The broad, relatively featureless absorption in the 600–900 nm region is characteristic of a porphyrin radical cation, whereas the ~1010 nm band is characteristic of the fullerene radical anion,[35,42] and the spectrum is assigned to the $P^{\bullet+}$–$C_{60}^{\bullet-}$ charge-separated state, formed *via* photoinduced electron transfer. The transient at 1000 nm features a prompt rise due to the porphyrin first excited singlet state, followed by an increase in absorbance with a time constant of 4.0 ps. This 4.0 ps increase is ascribed to formation of the $P^{\bullet+}$–$C_{60}^{\bullet-}$ charge-separated state. On a longer time scale (Fig. 11), the transient signal decays with a time constant of 20 ps, signaling recombination of the charge-separated state. Model porphyrin **3** has a lifetime for the first excited singlet state of 5.98 ns.[16] Thus, in **4** the rate constant for photoinduced electron transfer to give $P^{\bullet+}$–$C_{60}^{\bullet-}$ from ^{1}P (k_{ET}) is estimated to be (1/4.0 ps)–(1/5.98 ns), or 2.5×10^{11} s^{-1}. The quantum yield Φ of $P^{\bullet+}$–$C_{60}^{\bullet-}$ equals 1.0.

Fluorescence decay studies were also performed on films of **poly1** and **poly2** on ITO-coated glass electrodes in air. The film thickness was *ca.* 120 nm in both cases. Fig. 12 shows results with excitation into the Soret region at 430 nm (<10 pJ per pulse) and detection *via* a streak camera. The hollow circles show the results for **poly1**. The decay kinetics (shown at 680 nm) in the 590–830 nm region were fitted globally with exponential decays having lifetimes of 30 ps and 135 ps after deconvolution with the instrument response (20 ps FWHM). The inset in Fig. 12 shows the decay-associated spectra (DAS) of the emission of **poly1**, with maxima at *ca.* 670 and 690 nm. The major component at all wavelengths is the 30 ps decay. The spectra are very similar to those reported earlier for another sample of **poly1**,[16] but the major lifetime is somewhat longer (30 ps *vs.* 15 ps). This is likely because the previous sample was thinner, leading to the possibility of more rapid excited state quenching by the conductive electrode and surface defects. The amplitude of the longer-wavelength maximum relative to that at shorter wavelengths is greater in the 135 ps decay. This suggests that the 30 ps lifetime reflects in part migration of

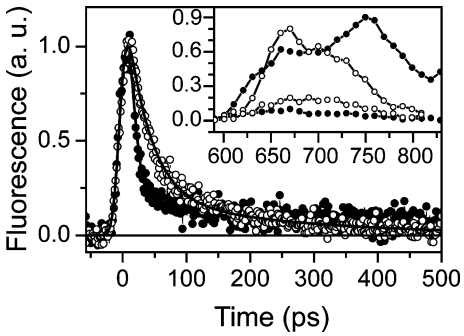

Fig. 12 Time resolved fluorescence data for **poly1** (open circles) and **poly2** (solid circles) films on ITO-coated glass in air, following excitation at 430 nm with a *ca.* 100 fs laser pulse. Detection was with a streak camera. The solid lines are exponential decays convoluted with the instrument response function, as explained in the text. The inset shows the DAS of the emissions, which have not been corrected for streak camera shading and spectral response.

excitation from higher- to lower-energy states that result from heterogeneity of the polymer. During the 135 ps decay, slower energy migration between chromophores of similar energy is likely occurring. The greatly shortened excited state lifetimes in **poly1** relative to that of model monomer **3** reflect efficient excited state quenching processes in the polymer sample. During migration excitons may be quenched by chemical and topological defects and exciton dissociation to charges within the polymer and at the conductive ITO surface. Lowering the temperature to 80 K did not significantly alter the fluorescence decay lifetimes (35 ps and 180 ps at 80 K) or amplitudes, showing that these decay mechanisms are not strongly activated processes.

Fig. 12 also shows the results of a similar experiment for **poly2** on an ITO-coated glass slide (solid symbols). The decay kinetics (shown at 750 nm) were fit globally in the 590–830 nm region with exponential decays having lifetimes of 7 ps and 200 ps, but the accuracy for the 7 ps component is not high given the strong convolution of the decay with the 20 ps streak camera response. The inset shows the corresponding DAS. The major, 7 ps DAS, has a maximum around 750 nm and a blue shoulder matching the fluorescence of **poly1**.

In the case of **poly2**, the lifetime of the vast majority of the porphyrin first excited singlet states is ~7 ps, which is much shorter than the lifetimes of these states in **poly1**. This lifetime is similar to the porphyrin excited state lifetime in model dyad **4** in solution, and the quenching is most likely due to photoinduced electron transfer to the fullerene to yield $P^{\bullet+}$–$C_{60}^{\bullet-}$, as was observed in **4**. The nature of the emission with the 750 nm maximum is not completely clear. Fullerenes in solution show fluorescence in this general region but with two bands located around 715 nm and about 800 nm. It is possible that this emission is due to somewhat-shifted fullerene fluorescence that is drastically quenched from the usual excited singlet state lifetime of such a fullerene (*ca.* 1.3 ns) due to photoinduced electron transfer from the porphyrin to form $P^{\bullet+}$–$C_{60}^{\bullet-}$. Alternatively, it is possible that this emission is due to an exciplex or charge-transfer (CT) exciton formed between the porphyrin and a nearby fullerene moiety, possibly from an adjacent polymer strand, which relaxes to the $P^{\bullet+}$–$C_{60}^{\bullet-}$ charge-separated state. Porphyrin–fullerene exciplexes as precursors to charge-separated states have been reported previously for some porphyrin–fullerene molecules

in solution where the two chromophores are spatially very close to one another.[43] In any event, it is clear that in **poly2**, the majority of the excited states decay by photoinduced electron transfer to form $P^{\bullet+}$–$C_{60}^{\bullet-}$. The nature of the extremely weak, 200 ps emission is unknown.

In order to learn more about the properties of the polymers after excitation, transient absorption experiments were performed on the same films using the pump–probe technique with excitation at 600 nm (~10–100 nJ per pulse) to ensure negligible excitation of fullerene and minimal effects of exergonic excited-state energy migration between porphyrins in different environments that would lead to spectral shifts. The results of these experiments are difficult to interpret fully due to the presence of the conducting ITO substrate which can accept charges and quench excited states, the inability to study individual polymer strands in fluid solution, and the absence of ideal model compounds. However, some interesting results are summarized below.

Fig. 13 shows results for a film of porphyrin **poly1** after excitation with different energy densities per laser pulse (136, 74, 28 and 14 μJ cm^{-2}, in order of decreasing ΔA at the maximum). Detection was at 880 nm, which is a spectral region in which most of the absorbance is attributed to porphyrin radical cations (polarons and CT excitons) (see Fig. 8 and 11), although some absorbance due to Frenkel excitons (excited states) may also be present. Although the decays are nonexponential, they are fitted well with 4 exponential components: 1.3 ps, 17 ps, 270 ps and a component that does not decay on this time scale. Global fitting results at different laser energy densities are shown in the inset as the logarithm of the amplitude *vs.* the logarithm of the excitation energy density. It is obvious that at higher excitation powers a very rapidly decaying (1.3 ps) transient appears and two fast-decaying components of 1.3 ps and 17 ps dominate the kinetics. At lower powers the 270 ps and non-decaying components becomes relatively more important.

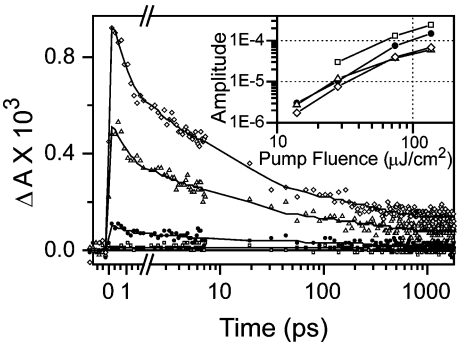

Fig. 13 Transient absorption kinetics at 880 nm for **poly1** on ITO-coated glass following excitation at 600 nm with 100 fs pulses. Decays shown, from maximum to minimum amplitude, were obtained with laser pulse fluences of 136, 74, 28, and 14 μJ cm^{-2}. The solid lines are multiple exponential decays fitted to the data as explained in the text. The inset shows amplitudes for these decays of 1.3 ps (open squares), 17 ps (filled circles), 270 ps (open triangles) and nondecaying on this time scale (open diamonds) obtained by global fitting of kinetics at the different laser pulse fluences.

At low excitation powers, the two decay components of 17 ps and 270 ps may be attributed mainly to the decay of porphyrin singlet excited states (*i.e.* Frenkel excitons) and the non-decaying component is attributed to radical cations (polarons) formed by electron transfer from porphyrin excited singlet states (*i.e.* dissociation of Frenkel excitons). The short lifetimes of the excited singlet states preclude significant triplet production by intersystem crossing, and even if some triplets are formed by singlet fission their transient spectral signature would appear at shorter wavelengths (<850 nm). This interpretation is consistent with the fluorescence lifetimes reported above.

As the laser power is increased, the fast components (1.3 and 17 ps) contribute proportionately more to the overall decay. Fig. 13 (see also ESI, Fig. S2‡) shows that none of 1.3 ps component is present at low laser powers, and none would have been apparent at the laser powers used for the time resolved fluorescence experiments described earlier. It is tempting to ascribe this fast decay to a process resulting from interaction of two excited states, such as exciton–exciton annihilation. However, calculations based on the excitation volume (*ca.* 8.3×10^{-9} cm^3), exciton density per laser pulse (*ca.* 7.9×10^{10} excitons per excitation volume at 136 μJ cm^{-2}), film absorbance, polymer density and volume per chromophore given above suggest that even at the center of the laser beam at highest fluence, there would be only about 1 photon absorbed for every 22 porphyrin chromophores. Singlet–singlet energy transfer rate constants are not known for the polymer. Time constants in other multiporphyrin arrays are typically on the order of tens of ps or longer, although time constants of a few ps are sometimes observed.[44–50] Thus annihilation seems unlikely here.

The transient results suggest that proportionately more new transients with higher extinction coefficients at 880 nm are generated at the higher laser powers very rapidly (approximately within the laser pulse), but that their decay times (*e.g.* 1.3 ps) are essentially independent of the laser pulse intensity. The reason for this behavior is unknown, but may be related to local heating (higher density of phonons) in the polymer at high laser powers leading to enhanced formation of CT excitons. Based on bulk spectroscopic and cyclic voltammetric measurements,[16] the energy of the porphyrin first excited singlet state of the porphyrin in **poly1** is 1.84 eV above the ground state, and the energy of the $P^{\bullet+}$–$P^{\bullet-}$ charge-separated state is 1.97 eV. Thus, photoinduced electron transfer would be slightly endergonic, and thermally activated. From the above results, photoinduced electron transfer does occur in the films, presumably to the ITO electrode and/or at local sites where the energy of the charge-separated state is lower. It may be that at high laser powers, local heating and perhaps melting (induced reversible "phase transition") of the polymer creates sites where the rate of charge separation is increased. In this case, the 1.3 ps decay component would be associated with the decay of CT excitons and all other decay components may be attributed mainly to the decay of radical cations (polarons) formed from those excitons.

As shown in the inset of Fig. 13, the amplitudes of the 17 ps, 270 ps and non-decaying components do not increase linearly with pump fluence. This behavior is consistent with a contribution from nongeminate recombination, which refers to recombination of electrons and holes generated by different photons at different charge-separation sites. (Geminate recombination refers to recombination of an electron and hole generated by a single photon at one charge-separation site, even though the electron and hole may

have separated spatially into different regions of the polymer prior to recombination.)

With this result as a background, we turn to the results for **poly2** (Fig. 14). The film thickness in this experiment is comparable to that used for Fig. 13. Spectra were obtained as explained above for **poly1**. Decays at 880 nm are nonexponential, but can be fitted well with 4 exponential components (4.6 ps, 56 ps, 670 ps and nondecaying on this time scale). The global fitting results are shown in the inset of Fig. 14. These results are all consistent with very fast decay of the porphyrin first excited singlet state by photoinduced electron transfer to yield $P^{\bullet+}$–$C_{60}^{\bullet-}$ charge-separated states (polarons and/or CT excitons), which decay over a variety of time scales. In contrast to **poly1**, no non-linear effects at high laser powers were observed.

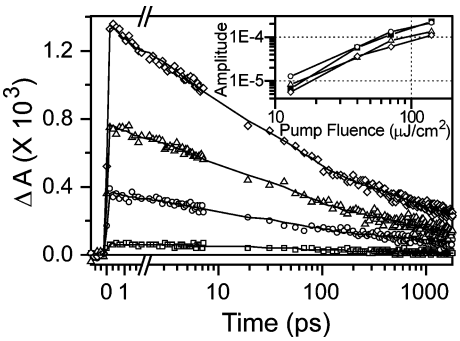

Fig. 14 Transient absorption kinetics at 880 nm for **poly2** on ITO-coated glass following excitation at 600 nm with 100 fs pulses. Decays shown, from maximum to minimum amplitude, were obtained with laser pulse fluences of 141, 71, 40, and 13 μJ cm^{-2}. The solid lines are multiple exponential decays fitted to the data as explained in the text. The inset shows amplitudes for these decays of 4.6 ps (solid squares), 56 ps (open circles), 670 ps (open triangles) and nondecaying on this time scale (open diamonds) obtained by global fitting of kinetics at the different laser pulse fluences.

The transient results suggest that most of the $P^{\bullet+}$–$C_{60}^{\bullet-}$ is formed on the time scale of the laser excitation pulse. This is consistent with the relatively small contribution of porphyrin emission to the emission spectra in Fig. 12. The 56 ps decay shows intensity-independent recombination dynamics (inset in Fig. 14), which is consistent with geminate recombination. Note that this lifetime is significantly longer than that observed for $P^{\bullet+}$–$C_{60}^{\bullet-}$ in model dyad **4** in solution (20 ps), suggesting that in the polymer, the electron and hole may migrate apart, on the same or different polymer chains, before recombination. The other lifetime components, especially the 4.6 ps component, show some deviation from first order kinetics, implying some nongeminate charge recombination. (At high charge densities, nongeminate recombination can be faster than geminate recombination). Note that although geminate recombination may or may not involve freely-diffusing charges, nongeminate recombination by its nature involves free mobile charges. The results also show that at all laser powers, some radical cations recombine on a much slower time scale than that employed for these studies.

3. Discussion

The electrochemical, spectroscopic and mass spectrometric results for **poly2** indicate that monomer **2** electropolymerizes oxidatively in a manner very similar to monomer **1** to produce a linear polymer with a polyporphyrin backbone, as in Fig. 2. The polymerization mechanism for both **1** and **2** is presumably related to that in polyaniline, and involves electrochemical preparation of an oxidized monomer radical cation which couples to a radical cation at the end of the growing polymer chain with the overall loss of 2 hydrogen ions. In accord with this mechanism, the polymerization solution becomes acidic as polymerization proceeds, with eventual protonation of the porphyrin macrocycles after a large number of CV scans.

The spectroscopic and electrochemical data show that in **poly2**, the porphyrin and fullerene chromophores retain their essential properties, rather than becoming part of a large delocalized π-electron system. The nitrogen-bearing aryl ring at a *meso*-position of each porphyrin is precluded from being coplanar with the macrocycle because of steric hindrance with the pyrrole β positions, and this allows only partial conjugation between the ring and the macrocycle, and hence along the polymer backbone. On the other hand, the various subunits of the polymer do interact, as evidenced by the red shifts and broadening of the absorption spectra and the change in electrochemical behavior of the porphyrin moiety upon polymerization. The first reduction potential of the fullerene, on the other hand, is essentially unchanged in **poly2** from its value in **2**, which is not unexpected, given the separation of this moiety from the polymer backbone.

The migration of positive charges ("holes") within the polymer films of both **1** and **2** and to the ITO surface clearly occurs. During polymerization, each oxidative CV sweep results in oxidation of all or most of the polymer porphyrins on the electrode surface, and then of monomer in solution so that polymerization can proceed. The CV results also show that in **poly2**, electrons can move through the film to the electrode. Because this occurs at potentials where the fullerene, but not the porphyrin, is reduced, it is likely that electron transfer occurs by hopping between C_{60} units along a polymer strand, and between strands. Thus, the film of **poly2** is both an electron conductor and a hole conductor. The IR results indicate that in the electrochemical experiment, oxidation is accompanied by migration of counterions from solution into the film, and that these counterions remain in the film until the film is returned to the neutral form.

The transient results show that the major pathway for decay of excitation in **poly2** is photoinduced electron transfer from the porphyrin to the fullerene to generate $P^{\bullet+}$–$C_{60}^{\bullet-}$. As shown in Fig. 15, both the porphyrin and fullerene first excited singlet states are thermodynamically capable of initiating electron transfer. Although the $P^{\bullet+}$–$C_{60}^{\bullet-}$ state can in principle recombine directly to the ground state, the transient absorption results for **poly2** suggest that some of the charge-separated states diffuse apart by hole migration through the porphyrin system and/or electron migration through the fullerene network before ultimately recombining.

The overall process in **poly2** is similar to that observed in "bulk heterojunction" organic photovoltaic cells. Such cells feature an intimate mixture of a conducting polymer phase and a fullerene electron transfer phase. In these cells, chromophore excited states (Frenkel excitons) decay by photoinduced electron transfer between the polymer phase and a nearby C_{60} derivative in the fullerene phase to form a charge-separated state (charge-transfer exciton). Given suitable energy, the electron and hole can then

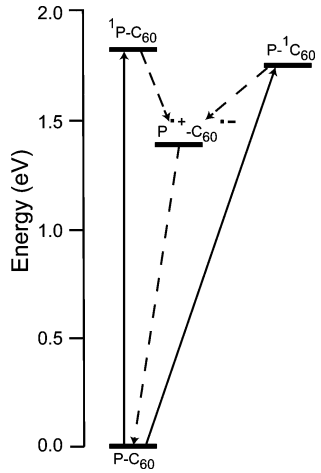

Fig. 15 Transient states and decay pathways for P–C_{60} units within **poly2**. Excited state energies are estimated from absorption spectra, and the energy of the charge-separated state is based on the electrochemical results. Competing with charge recombination of $P^{\bullet+}$–$C_{60}^{\bullet-}$ is migration of charge through the polymer network, and eventually to the ITO surface.

diffuse apart to give separated ions (exciton splitting). The free carriers (polarons) can then migrate to electrodes, giving rise to a photocurrent.

In **poly2** a similar process occurs. However, there is a major difference between the two systems. In the usual bulk heterojunction solar cell, light is absorbed by a chromophore in the polymer (or C_{60}) phase, and the resulting Frenkel exciton must diffuse to a boundary between the polymer and fullerene phases in order for charge transfer to occur. If this does not happen within the lifetime of the Frenkel exciton, it relaxes and the energy is lost as heat. **Poly2**, on the other hand, is constructed so that every porphyrin in the polymer backbone has a fullerene electron acceptor directly attached. In this "molecular heterojunction," photoinduced electron transfer to form a charge separated state can occur within a few ps after light absorption, and exciton migration is not required. Thus, one possible energy loss mechanism in the bulk heterojunction solar cell is eliminated. If **poly2** and similar polymers can be incorporated into photovoltaic cells that also feature high efficiency carrier migration and injection into electrodes, such polymers may be very useful for solar cell applications.

Acknowledgements

This work was supported by a grant from the US Department of Energy (DE-FG02-03ER15393). We gratefully acknowledge the use of facilities within the Center for Solid State Science at Arizona State University.

Notes and references

1 F. Bedioui, J. Devynck and C. Bied-Charreton, *Acc. Chem. Res.*, 1995, **28**, 30.
2 J. R. Fish, E. Kubaszewski, A. Peat, T. Malinski, J. Kaczor, P. Kus and L. Czuchajowski, *Chem. Mater.*, 1992, **4**, 795.
3 C. Poriel, Y. Ferrand, P. Le Maux, C. Paul-Roth, G. Simonneaux and J. Rault-Berthelot, *J. Electroanal. Chem.*, 2005, **583**, 92.
4 J. Basu and K. K. Rohatgimukherjee, *Sol. Energy Mater.*, 1991, **21**, 317.
5 D.-S. Duanmu, Z.-P. Chen, X.-S. Yu and X. Zhou, *Chin. J. Chem.*, 2004, **22**, 779.
6 D. Wohrle, *J. Porphyrins Phthalocyanines*, 2000, **4**, 418.
7 G. Li, S. Bhosale, S. Tao, R. Guo, S. Bhosale, F. Li, T. Zhang, T. Wang and J.-H. Furhop, *Polymer*, 2005, **46**, 5299.
8 C. Y. Lin, Y. C. Hung, C. M. Liu, C. F. Lo, Y. C. Lin and C. L. Lin, *Dalton Trans.*, 2005, 396.
9 K. A. Macor, Y. O. Su, L. A. Miller and T. G. Spiro, *Inorg. Chem.*, 1987, **26**, 2594.
10 A. Bettelheim, B. White, S. Raybuck and R. W. Murray, *Inorg. Chem.*, 1987, **26**, 1009.
11 A. Bettelheim, B. A. White and R. W. Murray, *J. Electroanal. Chem.*, 1987, **217**, 271.
12 A. Bettelheim, D. Ozer, R. Harth and R. W. Murray, *J. Electroanal. Chem.*, 1989, **266**, 93.
13 B. A. White and R. W. Murray, *J. Electroanal. Chem.*, 1985, **189**, 345.
14 E. M. Bruti, M. Giannetto, G. Mori and R. Seeber, *Electroanalysis*, 1999, **11**, 565.
15 S. Griveau, V. Albin, T. Pauporte, J. H. Zagal and F. Bedioui, *J. Mater. Chem.*, 2002, **12**, 225.
16 P. A. Liddell, M. Gervaldo, J. W. Bridgewater, A. E. Keirstead, S. Lin, T. A. Moore, A. L. Moore and D. Gust, *Chem. Mater.*, 2008, **20**, 135.
17 D. Gust and T. A. Moore, in *The Porphyrin Handbook*, ed. K. M. Kadish, K. M. Smith and R. Guilard, Academic Press, New York, 2000, vol. 8, ch. 57, pp. 153–190.
18 D. Gust, T. A. Moore and A. L. Moore, *Acc. Chem. Res.*, 2001, **34**, 40.
19 M. R. Wasielewski, *Chem. Rev.*, 1992, **92**, 435.
20 S. Fukuzumi and H. Imahori, *Electron Transfer in Chemistry*, 2001, 927.
21 D. M. Guldi, *Chem. Soc. Rev.*, 2002, **31**, 22.
22 H. Imahori, *Org. Biomol. Chem.*, 2004, **2**, 1425.
23 N. Martín, L. Sánchez, B. Illescas and I. Pérez, *Chem. Rev.*, 1998, **98**, 2527.
24 J.-F. Nierengarten, J.-F. Eckert, D. Felder, J.-F. Nicoud, N. Armaroli, G. Marconi, V. Vicinelli, C. Boudon, J.-P. Gisselbrecht, M. Gross, G. Hadziioannou, V. Krasnikov, L. Ouali, L. Echegoyen and S.-G. Liu, *Carbon*, 2000, **38**, 1587.
25 D. I. Schuster, *Carbon*, 2000, **38**, 1607.
26 T. J. Kesti, N. V. Tkachenko, V. Vehmanen, H. Yamada, H. Imahori, S. Fukuzumi and H. Lemmetyinen, *J. Am. Chem. Soc.*, 2002, **124**, 8067.
27 A. Cravino and N. S. Sariciftci, *J. Mater. Chem.*, 2002, **12**, 1931.
28 A. Cravino, *Polym. Int.*, 2007, **56**, 943.
29 J. Roncali, *Chem. Soc. Rev.*, 2005, **34**, 483.
30 D. Dubois, G. Moninot, W. Kutner, M. T. Jones and K. M. Kadish, *J. Phys. Chem.*, 1992, **96**, 7137.
31 M. E. Jamin and R. T. Iwamoto, *Inorg. Chim. Acta*, 1978, **27**, 135.
32 R. L. Hand and R. F. Nelson, *J. Am. Chem. Soc.*, 1974, **96**, 850.
33 T. F. Guarr and F. C. Anson, *J. Phys. Chem.*, 1987, **91**, 4037.
34 S. C. Paulson, S. A. Sapp and C. M. Elliott, *J. Phys. Chem. B*, 2001, **105**, 8718.
35 J. L. Bahr, D. Kuciauskas, P. A. Liddell, A. L. Moore, T. A. Moore and D. Gust, *Photochem. Photobiol.*, 2000, **72**, 598.
36 G. Kodis, P. A. Liddell, A. L. Moore, T. A. Moore and D. Gust, *J. Phys. Org. Chem.*, 2004, **17**, 724.
37 D. Kuciauskas, S. Lin, G. R. Seely, A. L. Moore, T. A. Moore, D. Gust, T. Drovetskaya, C. A. Reed and P. D. W. Boyd, *J. Phys. Chem.*, 1996, **100**, 15926.
38 D. Kuciauskas, P. A. Liddell, S. Lin, S. Stone, A. L. Moore, T. A. Moore and D. Gust, *J. Phys. Chem. B*, 2000, **104**, 4307.
39 P. A. Liddell, J. P. Sumida, A. N. Macpherson, L. Noss, G. R. Seely, K. N. Clark, A. L. Moore, T. A. Moore and D. Gust, *Photochem. Photobiol.*, 1994, **60**, 537.
40 P. A. Liddell, D. Kuciauskas, J. P. Sumida, B. Nash, D. Nguyen, A. L. Moore, T. A. Moore and D. Gust, *J. Am. Chem. Soc.*, 1997, **119**, 1400.
41 C. A. Reed and R. D. Bolskar, *Chem. Rev.*, 2000, **100**, 1075.
42 P. A. Liddell, G. Kodis, D. Kuciauskas, J. Andréasson, A. L. Moore, T. A. Moore and D. Gust, *Phys. Chem. Chem. Phys.*, 2004, **6**, 5509.
43 N. V. Tkachenko, L. Rantala, A. Y. Tauber, J. Helaja, P. H. Hynninen and H. Lemmetyinen, *J. Am. Chem. Soc.*, 1999, **121**, 9378.
44 N. Aratani, A. Osuka, H. S. Cho and D. Kim, *J. Photochem. Photobiol., C*, 2002, **3**, 25.

45 I.-W. Hwang, T. Kamada, T. K. Ahn, D. M. Ko, T. Nakamura, A. Tsuda, A. Osuka and D. Kim, *J. Am. Chem. Soc.*, 2004, **126**, 16187.
46 Y. Nakamura, I.-W. Hwang, N. Aratani, T. K. Ahn, D. M. Ko, A. Takagi, T. Kawai, T. Matsumoto, D. Kim and A. Osuka, *J. Am. Chem. Soc.*, 2005, **127**, 236.
47 A. Morandeira, E. Vauthey, A. Schuwey and A. Gossauer, *J. Phys. Chem. A*, 2004, **108**, 5741.
48 J.-S. Hsiao, B. P. Krueger, R. W. Wagner, T. E. Johnson, J. K. Delaney, D. C. Mauzerall, G. R. Fleming, J. S. Lindsey, D. F. Bocian and R. J. Donohoe, *J. Am. Chem. Soc.*, 1996, **118**, 11181.
49 S. Faure, C. Stern, R. Guilard and P. D. Harvey, *J. Am. Chem. Soc.*, 2004, **126**, 1253.
50 J. Larsen, J. Andersson, T. Polivka, J. Sly, M. J. Crossley, J. Sundstrom and E. Akesson, *Chem. Phys. Lett.*, 2005, **403**, 205.

